Control of Permanent-Magnet Synchronous Motors Using Fuzzy Logic Considering Parameter Variation and Diagnostic Capability For Hostile Environment Applications

Berhanu Deggefa Lemma, Srinivasan Pradabane
Department of Electrical Engineering, National Institute of Technology, Warangal, India.

***Abstract*— In this paper, the effect of parameter variation on the operation performance of the permanent magnet synchronous motor (PMSM) considered. The model which includes the parameter variation as a function of the operating condition is developed in MATLAB/Simulink. A non- linear control fuzzy logic control is used to dynamically change the control gain to regulate the toque dynamics while the fault information symptoms obtained from average park transformation is supplied to the fuzzy system to reveal the fault information. The simulation result indicates that the motor performance figure like ripple torque, ripple current and speed highly affected with parameter when parameter variation is considered.**

***Keywords*— permanent, magnet, synchronous, motor, fuzzy logic, parameter variation, diagnostic**

I. INTRODUCTION

Due to many advantages in terms of operational performance and reduction in loss due to no supply is required for rotor part permanent magnet synchronous motor attracts the researchers in different applications.

In [1] different control strategy like direct torque control (DTC) and phase variable approach is compared with vector control of PMSM. Techniques of control of PMSM has been discussed in [2] based on their significance for a specific application. Different control strategy is suited for different application. In a system where the overshoot, transient period and settling time is minimum, field-oriented control (FOC) is not the best option. A nonlinear control system was preferred compared to the linear control system. Model predictive control is the finest method of control from the existing nonlinear control system. When optimal segment to pole pitch, depth of air gap well designed, the AF-IPMSM has better performance compared to AF-SMPMSM in terms of ripple torque, total harmonic and power or torque ratio to volume [3]. Asymmetrical arranged wounded PMSM has a better performance in terms of cogging toque, harmonic and toque ripples compared to symmetrical arrangement [4]. The consequent pole magnet permanent motor has better performance than surface-mounted permanent magnet motor [5]. Induction machine has better performance in terms of cogging torque but the efficiency, power density and torque production of PMSM is improved [6]. Instantaneous voltage control scheme has good dynamic compared to direct torque control (DTC) as there is no sector identification is required [7]. For maximization of the drive performance and improved reliability due to switches failure, the redundant switches can be used [8]. Control of PMSM by field-oriented control (FOC), based on linear quadratic regulator (LQR) optimization has a good disturbance rejection with a considerable oscillation [9]. Fault detection by wavelet and Fourier analysis for the motor with a magnetic defect is performed in [10]. Open-end permanent magnet becomes the best option for high power electric drive due to its reliability and fault-tolerant operation [11]. Optimal current control that depends upon motor data is chosen to implement maximum torque per ampere (MTPA) [12]. Temperature affects both the resistance of stator and the demagnetization property of magnet [13].PI controller has a bottleneck like optimal coefficient setting that paves the way to look for non-linear control [14]. MTPA is mainly focused on minimization of input given, that the motor should produce a reference torque. When d axis and q axis inductance are not equal, d axis current is contributing to a torque dynamics [15]. Nonlinear controller is proposed to solve the difficult with the non-linear system [16]. Switching state, current ripple and measured current base predictive control of PMSM is done in [17]. In simple duty ratio regulated PMSM, switching period determines the magnitude of ripple and torque produced [18]. PMSM control using a nonlinear fuzzy logic to address the problem of torque ripple above synchronous speed operation area is considered in [19]. Fault diagnosis of PMSM of a machine based on fuzzy logic is covered in [20]. The simplest and easy way to detect the fault in the PMSM drive is using an average park vector by partitioning the range of fault symptoms, different fault was detected in [21], [22].

II. MATHEMATICAL MODEL OF PMSM

$$V_q = R * i_q + \frac{d}{dt}(\lambda_q) + \omega_s * \lambda_d \quad (1)$$

$$\lambda_d = L_d * i_d + \lambda_f \quad (2)$$

$$V_d = R * i_d + \frac{d}{dt}(\lambda_d) - \omega_s * \lambda_q \quad (3)$$

$$\lambda_q = L_q * i_q \quad (4)$$

$$\frac{d}{dt}(\omega_r) = \frac{T_e - T_L - B * \omega_r}{J} \quad (5)$$

$$\begin{matrix} V_a \\ V_b \\ V_c \end{matrix} = \begin{bmatrix} \cos(\theta r) & \sin(\theta r) & 1 \\ \cos(\theta r - 2/3 * \pi) & \sin(\theta r - 2/3 * \pi) & 1 \\ \cos(\theta r + 2/3 * \pi) & \sin co(\theta r + 2/3 * \pi) & 1 \end{bmatrix} * \begin{matrix} V_q \\ V_d \\ V_0 \end{matrix} \quad (6)$$

For generating a switching signal, the SVPWM is used. To reduce the effect of one axis flux on others voltage, the feed-

978-1-7281-8873-7/20/$31.00 ©2020 IEEE

forward component is added externally so that the parameters were detached from each other.

$$V_{dff} = -P * \omega r * L_q * i_q \quad (7)$$

$$V_{qff} = P * \omega r(L_d * i_d + \lambda f) \quad (8)$$

For supplying the drive the diode is used. Phase to neutral voltage is obtained from the pole voltage.

$$\begin{matrix} V_{an} \\ V_{bn} \\ V_{cn} \end{matrix} = \frac{2}{3} * \begin{bmatrix} V_{ao} \\ V_{bo} \\ V_{co} \end{bmatrix} - \frac{1}{3} * \begin{bmatrix} V_{bo} \\ V_{ao} \\ V_{ao} \end{bmatrix} - \frac{1}{3} * \begin{bmatrix} V_{co} \\ V_{co} \\ V_{bo} \end{bmatrix} \quad (9)$$

From the pole voltage the three phase to neutral voltage obtained by using the equation (9).

$$i_q = \frac{1}{L_q} \int (V_q - R * i_q - \omega_s * \lambda_d) dt \quad (10)$$

$$i_d = \frac{1}{L_d} \int (V_d - R * i_d + \omega_s * \lambda_q) dt \quad (11)$$

Torque developed by the PMSM, the speed and rotor angle is obtained by using the equations given below from equation (12) to equation (15).

$$T_e = 1.5 * P(\lambda_{ft} * i_q + (L_q - L_q) * i_q * i_d) \quad (12)$$

$$\omega_r = \frac{1}{J} \int (T_e - T_L - B * \omega_r) dt \quad (13)$$

$$\theta_r = \int \omega_r dt \quad (14)$$

$$\omega_s = P * \omega_r \quad (15)$$

When the magnitude of i_d is zero, the equation for V_d, V_q and T_e is reduced to a simple equation given below.

$$V_q = R * i_q + \omega_s * (\lambda_f) \quad (16)$$

$$V_d = -\omega_s * (L_q * i_q) \quad (17)$$

$$T_e = 1.5 * P(\lambda_f * i_q) \quad (18)$$

By comparing equation 12 and equation 18, taking the magnitude of $i_{q0} = \frac{T_{ref}}{1.5 * P * \lambda_f}$, the magnitude of the magnetic flux under at different current magnitude of current is estimated as it is given below.

$$\lambda_{ft} = \left(\frac{\lambda_f * i_{q0}}{i_q} + (L_d - L_q) i_d\right) \quad (19)$$

$$R_a = \frac{V_d * i_d + V_q * i_q - V_{q0} * i_{q0}}{{i_d}^2 + {i_q}^2 - {i_{q0}}^2} \quad (20)$$

III. CURRENT CONTROLLERS AND FAULT INFORMATION PROCESSING

The magnitude of the constant of controller for a current is obtained as it is written below [19].

$$\begin{matrix} kpd \\ kid \end{matrix} = \begin{matrix} kpq = \omega cc * L \\ kiq = \omega cc * R \end{matrix} \quad (21)$$

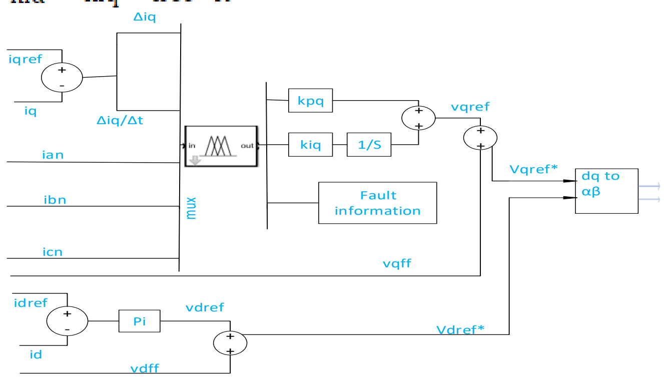

Fig 1 Current controller and fault information processing

For simplicity, the d-axis parameter is taken as it is. But for the q-axis, the gain is dynamically changed using the rate of current change and level of current deviation. The level of current deviation is taken from zero to maximum current (I_m) and rate of change is also taken as from zero to maximum current per second. Under normal operating condition the current of each phase approach to a sinusoidal wave. So the average current over one period is approximately 63.6% of the peak value of the current.

$$I_{av} = \frac{1}{2\pi} \int_0^T I_m \sin \omega t \, dt \quad (22)$$

A. Fuzzification And Inference System

The fuzzification procedure is completed by using a linguistic variable like negative giant (NG), negative average (NA), negative minor (NMI), null (NU), positive minor (PMI), positive average (PA), positive giant (PG). One symptom for fault occurrence is the change between nominal average value and real average value of a current. The second input to the fuzzy system is the parameter which indicates the place of the switch as the lower part of inverter or upper part of the inverter. Controller gain for q axis current is based on change and rate of change of current, when k_{Pd} and k_{iq} are variable defined by equation (21) [20].

TABLE 1 EXPERT SYSTEM FOR CHANGING K_{pq}

	$\frac{d\Delta i_q}{dt}$ (rate of change of iq)							
Δi_q	Value	NG	NA	NMI	NU	PMI	PA	PG
	NG	VVPG	VVPG	VPG	VPG	PG	PA	PA
	NA	VVPG	VPG	VPG	VPG	PG	PA	PA
	NMI	VVPG	VPG	VPG	PG	PA	VPMI	VPMI
	NU	VPG	VPG	PG	PA	PMI	VPMI	VPMI
	PMI	VPG	PG	PG	PMI	PMI	VPMI	NU
	PA	PA	PA	PMI	PMI	VPMI	VPMI	NU
	PG	PA	PA	PMI	VPMI	VPMI	NU	NU

TABLE 2 EXPERT SYSTEM FOR CHANGING k_{iq}

	$\frac{d(\Delta i_q)}{dt}$							
Δi_q	Value	NG	NA	NMI	NU	PMI	PA	PG
	NG	NU	NU	VPMI	VPMI	PMI	PA	PA
	NA	NU	VPMI	VPMI	PMI	PMI	PA	PA
	NMI	VPMI	VPMI	VPMI	VPMI	PA	PG	PG
	NU	VPMI	VPMI	PG	PG	VPG	VPG	VPG
	PMI	PMI	PMI	PA	PG	PG	VPG	VPG
	PA	PMI	PA	PMI	VPG	PA	VPG	VVPG
	PG	PA	PA	VPG	VPG	PA	VVPG	VVPG

B. Fault Information Processing

For a fault diagnosing, the fault symptom is required. For this purpose, the average park vector is used to drive fault symptoms. Fault symptoms which are used for detection purpose are an average current error (ACE) and average current (AC).

$$I_s = \sqrt{{i_d}^2 + {i_d}^2} \quad (23)$$

$$\begin{matrix} i_a \\ i_b \\ i_c \end{matrix} = i_m \begin{bmatrix} \sin(\omega s * t + \Phi) \\ \sin(\omega s * t + \Phi - \frac{2}{3} * \Pi) \\ \sin(\omega s * t + \Phi + \frac{2}{3} * \Pi) \end{bmatrix} \tag{24}$$

To simplify the diagnostic system, the three phase's current is normalized by taking the ratio of phase current by magnitude of Park's current.

$$\begin{matrix} i_{na} \\ i_{nb} \\ i_{nc} \end{matrix} = 1.5 * \frac{i_m}{|I_s|} \begin{bmatrix} \sin(\omega s * t + \Phi) \\ \sin(\omega s * t + \Phi - \frac{2}{3} * \Pi) \\ \sin(\omega s * t + \Phi + \frac{2}{3} * \Pi) \end{bmatrix} \tag{25}$$

$$\langle |i_{nj}| \rangle = \frac{\omega s}{2\Pi} \int_0^{\frac{2\Pi}{\omega s}} |i_{nj}| \, dt \tag{26}$$

From the average current and the nominal average under normal operating condition, the first fault symptom is obtained by taking their difference. During normal operation, the magnitude of ACE is near zero. So that the value approaches to zero is recommended to effectively identify the fault information. In addition to the first fault symptom, the average current is used as the second fault symptom to detect the location of a faulted switch.

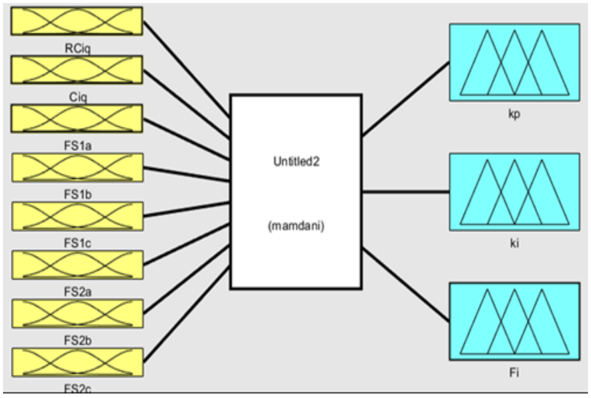

Fig 2 Fuzzy feed-forward FIS model of a system

By taking K1=0.06, K2 = 0.2, K0 =0.2 and dividing a range according to the equation given below the fuzzy rule is developed for fault detection.

$$FS1 = \begin{cases} A, & ACEj \le -K1 \\ B, & -K1 < ACEj \le K1 \\ B, & K1 < ACEj < \le K2 \\ D, & ACEj \ge K2 \end{cases} \tag{27}$$

$$\mathbf{FS2} = \begin{cases} E, & \langle inj \rangle < -K0 \\ F, & -K0 < \langle inj \rangle \le K0 \\ G, & \langle inj \rangle > K0 \end{cases} \tag{28}$$

The fault detection parameter can be arranged as it is stated in the table below [20], [21]. By taking the value of the controller constant (kp ki) obtained from equation 21, and limiting the value of Δi_q between -I_m to I_m and rate of $\frac{d\Delta i_q}{dt}$ between -I_m to I_m , the rules that relate the input to gain is developed. In addition by taking both the value of ACE (FS1) and AC (FS2) between -1 to 1 the rules that relate symptoms with fault information and fault point is developed.

TABLE 3 FAULTED SWITCHES AND SYMPTOMS COMBINATION

FS1a	FS1b	FS1c	FS2a	FS2b	FS2c	Faulted switches					
						S1	S2	S3	S4	S5	S6
C	A	A	E	-	-	X					
C	A	A	G	-	-		X				
A	C	A	-	E	-			X			
A	C	A	-	G	-				X		
A	A	C	-	-	E					X	
A	A	C	-	-	G						X
D	-	-	-	-	-	X	X				
-	D	-	-	-	-			X	X		
-	-	D	-	-	-					X	X
C	C	A	E	E	G	X		X			
C	C	A	G	G	E		X		X		
A	C	C	G	E	E			X		X	
A	C	C	E	G	G				X		X
C	A	C	E	G	E	X				X	
C	A	C	P	E	G		X				X
C	C	A	E	G	E	X			X		
C	C	A	G	E	G		X	X			
C	A	C	E	G	G	X					X
C	A	C	G	E	E		X			X	
A	C	C	E	E	G			X			X
A	C	C	G	G	E				X	X	

C. Simulation Results

PMSM model is developed in MATLAB/Simulink by considering parameter variation. The magnitude of controller constant for iq is changed to obtain good torque dynamic.

TABLE 4 SIMULATION PARAMETERS

Parameter	Magnitude
Resistor (ohm)	0.25
Inductance (mH)	5
Maximum current (A)	1.7
Controller bandwidth (rad/second)	1000
Frequency (Hz)	1000
Pole	10
Magnet flux (wb)	0.5
Torque (NM)	1

The Figure below demonstrates the simulation result considering a fixed magnetic flux and armature resistance

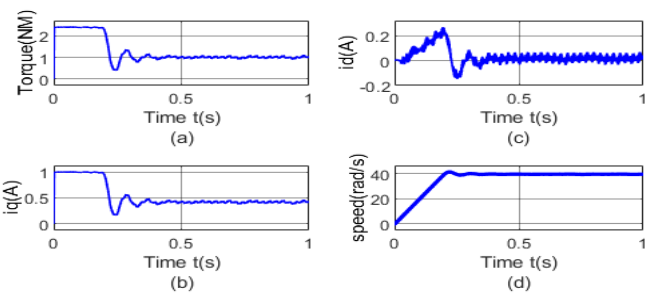

Fig 3 Simulation result without parameter variation: (a) Shows the torque, (b) shows the q-axis current, (c) shows direct axis current and (d) shows speed.

As it has appeared above on Fig 3(a), the torque is ripple is mainly affected by q axis current. Fig 3 (c) and 3(d) delineate that both d axis and speed settle quickly to steady-state.

Fig 4 depicted below shows a simulation by considering parameter variation as it is written in equation 19 and 20.

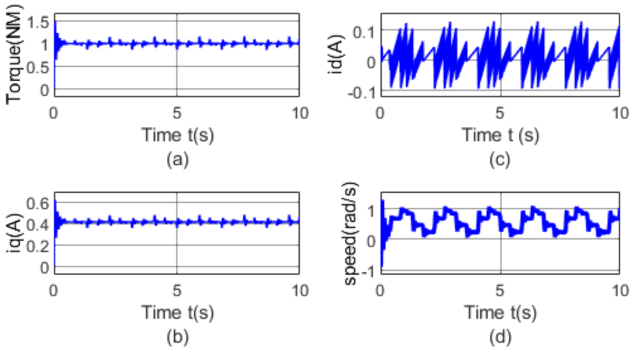

Fig 4 Simulation result with parameter: (a) Shows the torque, (b) shows the q-axis current, (c) shows direct axis current and (d) shows speed

As shown on Fig 4 (a) the magnitude of harmonic on torque is high when parameter variation is considered. From Fig 4(c) and Fig 4(d), it can be observed that both d axis current and speed is highly affected by variation that occurs in magnetic flux and armature resistance.

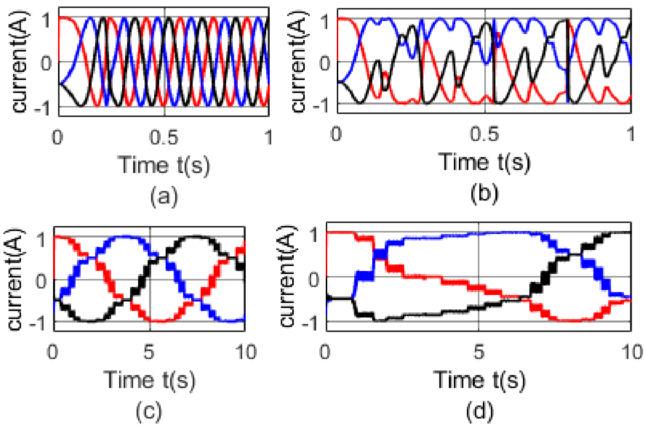

Fig 5.Normalized current: (a) is a current with a fixed parameter, (b) is current with a fixed parameter when S1 is opened, (c) is a current with parameter variation, and (d) is a current with parameters variation when S1 is opened.

From Fig 5(c), above diagram, it is clearly seen that even under normal operating condition, the voltage harmonics occur due to variation in a magnetic flux when the model with parameter variation is considered.

IV. CONCLUSION

Mathematical model of a PMSM developed including the magnetic nonlinearity in magnetic and resistance variation due to the current flowing through a winding. Per unit average obtained from park transformation is used for identifying and locating a fault. Fault identification rule is developed according to the table 3. The fault detection is done by using the fuzzy inference system using a Mamdani system. To control the motor torque, the controller constant of i_q is changed according deviation in average current and rate of deviation. When the parameter variation is included, the performance of a parameter is different from the model that developed assuming the fixed parameter. When the motor is modeled including the parameter variation, the torque ripple is high. In addition to this, the current ripple and speed ripple is also high compared to the fixed-parameter model.

V. REFERENCE

[1]. Veena, V. S., Chari, S., Ravichandran, M. H., & Praveen, R. P. (2014, March). Vector control of three phase PMSM drive using power transformations for future spacecraft application. In 2014 International Conference on Circuits, Power and Computing Technologies [ICCPCT-2014] (pp. 313-319). IEEE.

[2]. Bida, V. M., Samokhvalov, D. V., & Al-Mahturi, F. S. (2018, January). PMSM vector control techniques—A survey. In 2018 IEEE Conference of Russian Young Researchers in Electrical and Electronic Engineering (EIConRus) (pp. 577-581). IEEE.

[3]. Aydin, M., & Gulec, M. (2016). A new coreless axial flux interior permanent magnet synchronous motor with sinusoidal rotor segments. IEEE Transactions on magnetics, 52(7), 1-4.

[4]. Demir, Y., & Aydin, M. (2016). A novel dual three-phase permanent magnet synchronous motor with asymmetric stator winding. IEEE Transactions on Magnetics, 52(7), 1-5.

[5]. Onsal, M., Demir, Y., & Aydin, M. (2017). A new nine-phase permanent magnet synchronous motor with consequent pole rotor for high-power traction applications. IEEE Transactions on Magnetics, 53(11), 1-6.

[6]. Dobzhanskyi, O., Amiri, E., & Gouws, R. (2016, October). Comparison analysis of electric motors with two degrees of mechanical freedom: PM synchronous motor vs induction motor. In 2016 II International Young Scientists Forum on Applied Physics and Engineering (YSF) (pp. 14-17). IEEE.

[7]. Kumar, K. R., Nithin, K., & Kumar, T. V. (2016, November). Torque ripples reduction in PMSM drive based on instantaneous voltage control technique. In 2016 IEEE 7th Power India International Conference (PIICON) (pp. 1-6). IEEE.

[8]. Kolli, A., Béthoux, O., De Bernardinis, A., Labouré, E., & Coquery, G. (2013). Space-vector PWM controls synthesis for an H-bridge drive in electric vehicles. IEEE Transactions on Vehicular Technology, 62(6), 2441-2452.

[9]. Xia, C., Liu, N., Zhou, Z., Yan, Y., & Shi, T. (2018). Steady-state performance improvement for LQR-based PMSM drives. IEEE Transactions on Power Electronics, 33(12), 10622-10632.

[10]. Ishikawa, T., Seki, Y., & Kurita, N. (2013). Analysis for fault detection of vector-controlled permanent magnet synchronous motor with permanent magnet defect. IEEE transactions on magnetics, 49(5), 2331-2334.

[11]. Wang, J., & Wu, J. (2016, October). Space Vector Modulation Based on Lookup Table for a Dual-Inverter-Fed Open-End Winding PMSM Drive. In 2016 IEEE Vehicle Power and Propulsion Conference (VPPC) (pp. 1-6). IEEE.

[12]. Jiang, W., Feng, S., Zhang, Z., Zhang, J., & Zhang, Z. (2018). Study of Efficiency Characteristics of Interior Permanent Magnet Synchronous Motors. IEEE Transactions on Magnetics, 54(11), 1-5.

[13]. Zhang, Z., Li, G., Qian, Z., Ye, Q., & Xia, Y. (2016, June). Research on effect of temperature on performance and temperature compensation of interior permanent magnet motor. In 2016 IEEE 11th Conference on Industrial Electronics and Applications (ICIEA) (pp. 411-414). IEEE.

[14]. Wang, Q., Yu, H., Wang, M., & Qi, X. (2019). An improved sliding mode control using disturbance torque observer for permanent magnet synchronous motor. IEEE Access, 7, 36691-36701.

[15]. Li, K., & Wang, Y. (2018). Maximum torque per ampere (MTPA) control for IPMSM drives based on a variable-equivalent-parameter MTPA control law. IEEE Transactions on Power Electronics, 34(7), 7092-7102.

[16]. Xue, Y., Yu, H., & Liu, X. (2019). Improved Fuzzy Backstepping Position Tracking Control for Manipulator Driven by PMSM. In 2018 Chinese Automation Congress (CAC) (pp. 3561-3565). IEEE

[17]. Zanma, T., Tozawa, S., Takagi, Y., Koiwa, K., & Liu, K. Z. (2020). Optimal voltage vector in current control of PMSM considering torque ripple and reduction of the number of switching operations. IET Power Electronics, 13(6), 1200-1206.

[18]. Adase, L. A., Alsofyani, I. M., & Lee, K. B. (2019). Predictive Torque Control with Simple Duty-Ratio Regulator of PMSM for Minimizing Torque and Flux Ripples. IEEE Access.

[19]. Wang, C., & Zhu, Z. Q. (2020). Fuzzy Logic Speed Control of Permanent Magnet Synchronous Machine and Feedback Voltage Ripple Reduction in Flux-Weakening Operation Region. IEEE Transactions on Industry Applications, 56(2), 1505-1517.

[20]. Yan, H., Xu, Y., Cai, F., Zhang, H., Zhao, W., & Gerada, C. (2018). PWM-VSI fault diagnosis for a PMSM drive based on the fuzzy logic approach. IEEE Transactions on Power Electronics, 34(1), 759-768.

[21]. Sital-Dahone, M., Saha, A., Sozer, Y., & Mpanda, A. (2017, March). Multiple device open circuit fault diagnosis for neutral-point-clamped inverters. In 2017 IEEE Applied Power Electronics Conference and Exposition (APEC) (pp. 2605-2609). IEEE.

[22]. Ubale, M. R., Dhumale, R. B., & Lokhande, S. D. (2013). Open switch fault diagnosis in three phase inverter using diagnostic variable method. International journal of research in engineering and technology, 2(12), 636-641.